Iranian Journal of Electrical and Electronic Engineering 04 (2022) 2514
Microgrid Special Issue 2022: Operation, Control, and Applications

Iranian Journal of Electrical and Electronic Engineering

Journal Homepage: ijeee.iust.ac.ir

Research Paper

Load Profile Flattening Considering EV's Initial and Final SoC and Arrival and Departure Times

V. Bagheri*, A. F. Ehyaei*(C.A.), and M. Haeri**

Abstract: In distribution networks, failure to smooth the load curve leads to voltage drop and power quality loss. In this regard, electric vehicle batteries can be used to smooth the load curve. However, to persuade vehicle owners to share their vehicle batteries, we must also consider the owners' profits. A challenging problem is that existing methods do not take into account the vehicle owner demands including initial and final states of charge and arrival and departure times of vehicles. Another problem is that battery capacity of each vehicle varies depending on the type of vehicle; which leads to uncertainties in the charging and discharging dynamics of batteries. In this paper, we propose a modified mean-field method so that the load curve is smoothed, vehicle owner demands are met, and different capacities of electric vehicle batteries are considered. The simulation results show the effectiveness of the proposed method.

Keywords: Load profile, Wind turbine, Photovoltaic, State of Charge, Electric vehicle.

1 Introduction

IN recent years, due to the growing interest in renewable energy resources, a lot of small wind turbines (WTs) and photovoltaics (PVs) have been manufactured for installation in homes. Meanwhile, electric vehicles (EVs) have been produced extensively due to their high efficiency, lower cost, and less fuel pollution. However, failure to smooth the charge of electric vehicle batteries and the output power of wind turbines and photovoltaics causes voltage peak, power quality loss, and voltage deviation in the network.

Iranian Journal of Electrical and Electronic Engineering, 2022.
Paper first received 14 May 2022, revised 31 Oct 2022, and accepted 04 Nov 2022
*The authors are with the Electrical Engineering Department Faculty, Imam Khomeini International University, Qazvin, Iran.
E-mails: V.Bagheri@edu.ikiu.ac.ir, and f.ehyaei@eng.ikiu.ac.ir.
** The authors are with the Electrical Engineering Department Faculty, Sharif University of Technology, Tehran, Iran.
E-mails: haeri@sharif.ir
Corresponding Author: A. F. Ehyaei.
https://doi.org/10.22068/IJEEE.18.4.2514

As a result, different methods are used to smooth the load curve; the most common methods [1] are peak shaving, valley filling, and load shifting (Fig. 1).

The peak shaving method is one of the most common load management methods that reduce the peak demand. The valley filling method aims to reduce the level of load difference between peak load and valley load. The shifting load method is mostly used in demand-side management. This method is the most effective load management method that shifts the load from peak hours to off-peak hours by combining valley filling and peak shaving methods [2].

Time-varying load has been used in demand-side management in [3]. Using peak shaving and shifting load methods helps the distribution network to reduce peak demand and electricity energy billing costs. A diesel generator, a wind turbine, consumption load, dump load, and a battery are used in [4]. Diesel generator and wind control enable the battery to smooth wind and load variation; so that the power quality of the islanded system is improved.

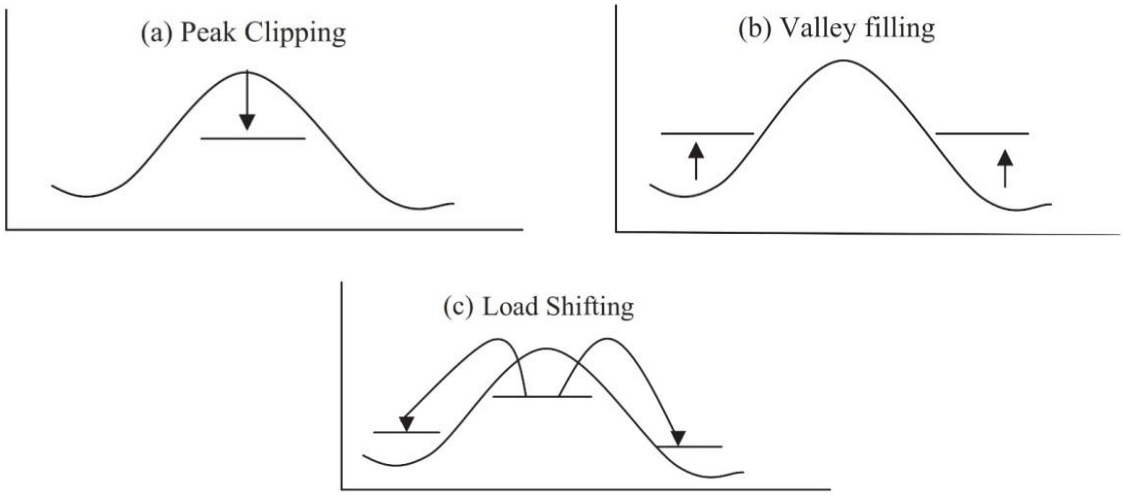

Fig. 1 A variety of methods of load curve flattening.

The battery is also used for frequency regulation and peak shaving. Peak load shaving opportunities in district heating systems have been analyzed in [5]. It also examines the effect of variation in the heat demand of buildings or the installation of local storage systems on the total load. Battery storage potential has been used for peak shaving in low voltage distribution networks focusing on residential areas in [6]. For the effects of high penetration of renewable energy sources in the power system, battery storage has been used to peak load shaving and load curve smoothing in [7]. To reduce the stress on the power distribution network and increase the profits of PV owners, increase self-consumption and peak shaving of home photovoltaics using batteries and curtailment [8]. In [9] using batteries for peak cutting, the payback period shortens large industrial loads, and the effect of peak shaving on the return of investment and the aging of the battery is shown. An optimal peak shaving strategy is proposed for an energy storage system to reduce peak demand consumption in [10]. Also, a cost-savings analytical tool has been created for customers to choose the right size of energy storage for various tariff schemes. In [11], the load curve of the system consisting of diesel generators, PV farms, and batteries in island mode based on load forecasting smoothed and shaved the peak load curve. In [12], a battery is used simultaneously for optimization of peak shaving and frequency regulation, including battery degradation, operating constraints and load uncertainties, and regulation signals.

An energy management system has been proposed to consider energy consumption and production simultaneously to reduce energy costs in [13]. The scheduling method in a typical home includes various home appliances, a small wind turbine, a PV panel, and a battery in 24 hours. In [14], the effects of electric vehicles for peak shaving and valley filling, the effects of electric vehicles on the grid (V2G), and the effects of the grid on electric vehicles (G2V) on dynamic economic/emission dispatch have been investigated. The uncoordinated charging of many electric vehicles increases the peak load during rush hours and challenges the stability and security of the power grid [15]. If the number of electric vehicles involved is more than one million; a highly efficient valley-filling strategy is used, which has two indices: capacity margin index and charging priority index. In [16], peak shaving and valley filling methods in the power consumption profile have been used to schedule the charging and discharging of electric vehicles in the parking lots. In this method, the profile of power consumption during the day is smoothed, and as a result, the cost of electricity is reduced; this reduction is very important for electricity consumers. The uncoordinated charging load in many electric vehicles increases the gap between peak load and valley load. Appropriate battery charging pricing mechanisms have been used to reduce the negative effects of uncoordinated battery charging, assist the power grid in valley load, and increase social welfare in [17]. The demand response is done using the Stackelberg game to balance supply and demand and smooth the aggregated load [18]. The proposed method has met consumers' demand, including peak demand smoothing valley filling and reducing the mismatch between supply and demand.

A distributed algorithm for sparse load shifting is proposed to reduce energy costs, daily peak demand,

and customer discomfort and solve the problem of scheduling residential smart appliances [19]. A new algorithm for charging and discharging batteries for peak load shaving, power curve smoothing, and voltage regulation of a distribution transformer using load forecasting has been proposed in [20]. Time-of-use (TOU) energy cost management using batteries is provided to reduce electricity bills [21]. The application of TOU is economically useful when there is a large difference between the maximum and minimum electricity prices. In [22], the Internet of Things (IoT) is used for peak load shifting by end-users in the market; users can charge and discharge energy storage facilities to reduce operating costs.

The demand response presented in [23] manages the demand-side resources in real-time. In this method, due to supply fluctuations, electricity demand changes. If integrated with electricity markets, demand response can be used for load shifting and as an alternative to reserve control and balancing energy. The purpose of the strategy in [24] is to identify the connection status of each battery and the sequence priority between batteries. This strategy manages batteries through seven operating modes; which provide power exchange between batteries and the power grid, especially during rush hours, and load power variance minimizes to smooth the power demand curve and reduce the stress of the power grid.

According to above studies, the cost functions related to different load management methods are based on minimizing the cost of electricity and maximizing the profit of the distribution network. However, if we want the customer to provide us with his car battery, we must also consider the customer's profit.

The innovation of the present work is:

A modified algorithm is presented to optimize the charge and discharge of batteries in load curve flattening problems with met customer requirements.

To this end, the rest of the paper is organized as follows: Section 2 introduces the network, network components and the connection strategy of renewable energy resources, electric vehicles, and loads. In this section, to consider the profit of vehicle owners, four parameters of arrival & departure times and initial & final SoC are introduced. In section 3, the cost function and the optimization problem are defined and a new method based on mean-field algorithm is presented to smooth the load curve. In section 4, the amount of renewable energy production, cost function parameters, battery capacity of different vehicles and also vehicle demands are quantified and the simulation results are given. Finally, concluding remarks are provided in section 5.

2 System Description

Home customers fall into three categories (Fig. 2). The first category only contains loads. The second category, in addition to the load, has a small wind turbine. The third category, in addition to the load, has photovoltaics as well. Customers get part of their power from renewable energy resources such as home-installed wind turbines or photovoltaics in the second and third categories. Electric vehicle batteries are connected to the distribution network, either in the parking lot or at home. When a battery is connected to the grid, it declares four parameters: arrival time, departure time, initial SoC, and final SoC. The aggregator smooths the load curve considering the output power of the wind turbine, the output power of the photovoltaic, and the required power for the home load and taking into account of the connected batteries declaration.

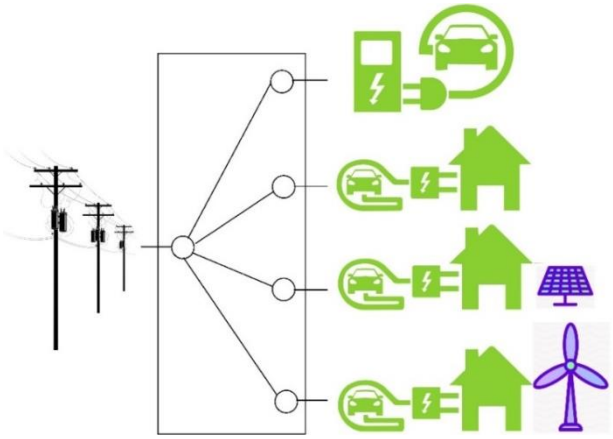

Fig. 2 Types of connection of electric vehicles to the distribution network.

Total home power consumption and total production capacity of renewable resources for the customer $n \in N$ at $t \in T$ are considered as $p_n^{D,t}$ and $p_n^{S,t}$, respectively. As a result, the total uncontrollable power for each customer is considered as $p_n^{Un,t} = p_n^{D,t} - p_n^{S,t}$. Production capacity of renewable resources for customer $n \in N$ at $t \in T$ is considered as $p_n^{S,t} = p_n^{PV,t} + p_n^{WT,t}$. The previous days' uncontrollable power curve is used as a power forecast for the following days. Then, the total customer power, including EV battery, is determined as follows:

$$p_n = p_n^{Un} + \gamma_n (q_n^C - q_n^D), \quad (1)$$

$$\gamma_n = \begin{cases} 1, & t_{arr}^n \le t \le t_{dep}^n \\ 0, & O.W \end{cases}$$

where variables are $p_n^{Un} = [p_n^{Un,1} \quad \cdots \quad p_n^{Un,T}]^T$, $p_n = [p_n^1 \quad \cdots \quad p_n^T]^T$, $q_n^C = \left[q_n^{C,1} \quad \cdots \quad q_n^{C,T}\right]^T$, and $q_n^D = [q_n^{D,1} \quad \cdots \quad q_n^{D,T}]^T$. $q_n^{C,t}$ and $q_n^{D,t}$ indicate the charge and discharge of the n^{th} battery at $t \in T$. Electric vehicles arrival and departure times are denoted by t_{arr}^n and t_{dep}^n respectively. γ_n is defined for the n^{th} EV according to its arrival and departure times.

We consider the dynamics of SoC as follows [25]:

$$s_n^t = s_n^{t-1} + \frac{\mu_n}{\varsigma_n} q_n^{C,t} - \frac{\mu_n^{-1}}{\varsigma_n} q_n^{D,t} \tag{2}$$

μ_n and ς_n is show charging efficiency and battery size, where the following constraints and initializations are in order.

$0 \le s_n^t \le 1$, $0 \le q_n^{C,t} \le q_n^{C,\max}$, $0 \le q_n^{D,t} \le q_n^{D,\max}$, $s_n^{t_0^n} = SoC_0^n$, $t_0^n = t_{arr}^n$, $s_n^{t_F^n} = SoC_F^n$, $t_F^n = t_{dep}^n$.

s_n^t indicates the SoC of customer n at time t and SoC_0^n and SoC_F^n represent initial and final values of the SoC.

Note that for $\gamma_n = 0$, the amount of charge and discharge of the battery is assumed to be zero, and we solve the defined optimization problem without considering all the constraints in (2). However, if $\gamma_n = 1$, then all constraints in (2) are considered.

3 Optimization Problem and the Proposed Method of Load Flattening

Now, the price function is considered as follows [25]:

$$T_n^t(p_n^t, \bar{p}^t) = a_{e,n}^t p_n^t + b_e^t \bar{p}^t + c_e^t \tag{3}$$

where $a_{e,n}^t \ge 0$ and $b_e^t > 0$, and $\bar{p}$ is defined as

$$\bar{p} = \sum_{n \in N} \frac{1}{N} p_n \tag{4}$$

where $\bar{p}$ is $\bar{p} = [\bar{p}^1, \quad \cdots, \quad \bar{p}^T]^T$. $a_{e,n}^t$, b_e^t, and c_e^t are predetermined. The price function in (3) is effective in moving the load (due to the dependence of the price function on $\bar{p}^t$) and reducing the load (due to the dependence of the price function on p_n^t). According to the price function for customer n, the daily bill is calculated as follows [25]:

$$E_n^t(p_n^t, \bar{p}^t) = T_n^t(p_n^t, \bar{p}^t) p_n^t \tag{5}$$

Term $a_{e,n}^t p_n^t$ in the price function converts the electricity bill into a quadratic form, encouraging customers to reduce consumption. Term $b_e^t \bar{p}^t$ also encourages customers not to consume during peak rush hours, and it helps to smooth the load curve. Term c_e^t is for changing electricity tariffs at different times of the day by the distribution network. The cost of degradation of electric vehicle batteries is considered as follows [25]:

$$H_n(q_n^t) = a_{h,n}\left(\left(q_n^{C,t}\right)^2 + \left(q_n^{D,t}\right)^2\right) + b_h(q_n^{C,t} + q_n^{D,t}) \tag{6}$$

where $q_n^t = \left[q_n^{C,t} \quad q_n^{D,t}\right]^T$. Therefore, the n^{th} customer cost function is defined as:

$$U_n(q_n, \bar{p}) = \sum_{t \in T} (E_n^t(p_n^t, \bar{p}^t) + \gamma_n H_n(q_n^t)) \tag{7}$$

here q_n is $q_n = [q_n^C \quad q_n^D]^T$. The main task for each customer is to obtain the optimal value of q_n to minimize the cost function in (7).

According to (7), each customer's strategy affects other customers through $\bar{p}^t$. Also, since each player in the game does not have information about the strategy of other players, this game is not complete with information. However, since $\bar{p}$ is a common term in the cost function of all players, players do not need to know the optimal strategy of other players. As a result, a modified decentralized mean-field optimization is proposed to solve the problem. In this method, information does not exchange among the players, but is only communicated between the players and the distribution network. That is, the distribution network calculates the optimal strategy for the players and sends the estimated amount to all of them. In other words, aggregator calculates the mean field term and estimates the next level for this term. Thus the common term $\bar{p}$, called the mean-field term, is estimated by $z(k)$, where k is the step number of the algorithm. By employing $z(k)$ instead of $\bar{p}$, The optimization problem for the n^{th} player is modified as follows [25].

$$q_n^*(z(k)) = \underset{q_n}{\operatorname{argmin}}\, U_n(q_n, z(k)) \tag{8}$$

Using the Mann iteration algorithm [26], the update rule is defined as [25]:

$$z(k+1) = (1 - \lambda(k))z(k) + \lambda(k)\Lambda(z(k)),\ \Lambda(z(k)) = \textstyle\sum_{n \in N} \frac{1}{N} p_n^*(z(k)) \tag{9}$$

where $\sum_{k=0}^{\infty} \lambda(k) = \infty$ and $\sum_{k=0}^{\infty} \lambda(k)^2 < \infty$ and for every iteration k we consider $p_n^*(z(k)) = p_n^{Un} + \gamma_n \left(q_n^{C*}(z(k)) - q_n^{D*}(z(k))\right)$.

The estimation and optimization process is described through the following algorithm.

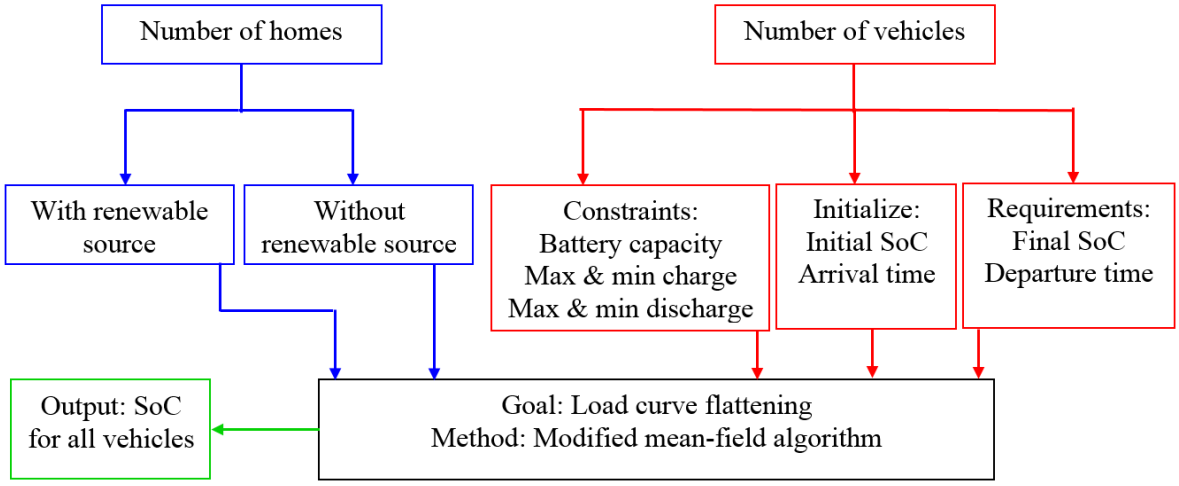

Fig. 3 Flowchart of the proposed method.

According to this algorithm, each player plans his optimal strategy using the average network consumption. Then, according to the consumption curve of the players in different iterations, estimate of the average network load curve is updated by the distribution network and sent to the players. If customer n cannot send its corresponding p_n value at any iteration, the algorithm continues with the last p_n value sent by the player. In the remaining of this section, a modified mean-field algorithm is presented using the modified cost function and the modified $p_n^*(z(k))$ compared to the original mean-field algorithm. The flowchart of the proposed method is shown in Fig. 3.

Modified mean-field algorithm for electric vehicle charging problem:

initialization
  randomly initialize $z(0), k \leftarrow 0$
iteration
  for $n \in N$
    $q_n^*(z(k)) \leftarrow \underset{q_n}{\operatorname{argmin}}\, U_n(q_n, z(k))$
    $p_n^*(z(k)) \leftarrow p_n^{Un} + \gamma_n(q_n^{C*}(z(k)) - q_n^{D*}(z(k)))$
  end
    $\Lambda(z(k)) \leftarrow \sum_{n\in N} \frac{1}{N} p_n^*(z(k))$
    $z(k+1) \leftarrow (1-\lambda(k))z(k) + \lambda(k)\Lambda(z(k))$
    $k \leftarrow k+1$

Lemma 1: According to Theorem 3 in [25], if the assumptions of Theorem 2 in [25] are valid and the population of players converges infinitely, then the proposed algorithm converges to the Nash equilibrium point.

4 Simulation and Results

In the first of this section, different values of system components and parameter values are given. The load consumption of homes is borrowed from [27]. The predicted output power of the photovoltaic and wind turbine are employed in Table 1 from [28]. In this table, the output power is given based on the power of the installed units. The installed power of photovoltaic and wind turbines in this article is 1kW. The output power of the photovoltaic and wind turbine and the load consumption of homes is based on the table, and the power of the installed units for renewable resources is given in Table 1. For the feasibility of the problem, the load consumption of homes is considered quintuple of the curve from [27]. For all the customers, the values of the load consumption of homes and the power of the renewable resources are randomly generated for each hour from the normal distribution with mean parameter mu and standard deviation parameter sigma, that mu is equal to the value corresponding to the same hour in Table 1 and sigma is equal to 0.1.

Parameters are selected as $a_{e,n}^t = 1000$, $b_e^t = 13.5$, $c_e^t = 0$, $a_{h,n} = 1.2$, $b_h = 0$, and $\mu_n = 0.95$. The battery capacity of each vehicle is employed as in [29]. These values are given in Table 2. ς_n is chosen from the column battery capacity in Table 2.

To evaluate the modified algorithm, three different scenarios are considered. The details of these three scenarios are given in Table 3. In each scenario, the average number of vehicles of different types, the number of home loads without renewable

resources, the number of home loads with PV, the number of home loads with WT, the number of vehicles located in parking lots, the arrival time of batteries and the departure time of batteries are given.

Table 1 Output power of photovoltaic and wind turbine.

Hour	Power of photovoltaic (kW)	Power of wind turbine (kW)	Load consumption of home (kW)
1	0	0.119	13.1
2	0	0.119	10.9
3	0	0.119	9.65
4	0	0.119	9.5
5	0	0.119	8.85
6	0	0.061	8.95
7	0	0.119	9.45
8	0.008	0.087	9.25
9	0.15	0.119	8.75
10	0.301	0.206	9.15
11	0.418	0.585	10.55
12	0.478	0.694	10.075
13	0.956	0.261	13.35
14	0.842	0.158	7.8
15	0.315	0.119	8.35
16	0.169	0.087	8.55
17	0.022	0.119	8.65
18	0	0.119	9.2
19	0	0.0868	9.375
20	0	0.119	9.85
21	0	0.0867	10.15
22	0	0.0867	9.235
23	0	0.061	10.15
24	0	0.041	15

Table 2. Types of vehicles and battery capacity of each vehicle.

Brand	Model	Battery capacity (kWh)	$q_n^{C,\max}, q_n^{D,\max}$ (kWh)
Chevrolet	Spark EV	18.3	7.32
Honda	FIT	20	8
Fiat	500e	24	9.6
BMW	i3	27.2	10.88
Mercedes	B250e	28	11.2
Ford	Focus-e	33.5	13.4
Hyundai	Ioniq-e	38.3	15.32
Nissan	LEAF	40	16
Toyota	RAV4	41.8	16.72
Kia	Soul EV	64	25.6
Tesla	Model 3	78	31.2

The minimum time between arrival and departure time is 2 hours. There is no limit to the choice between the minimum time of arrival and departure of batteries. However, if the minimum time between arrival and departure time is more than one; the total load curves of this system are very close to each other. Usually, the initial SoC of batteries when connected to the network may be any value between zero to one. For this reason, the initial SoC of batteries at arrival time is randomly considered in the interval [0,1]. Also, the requested charge for each car when disconnected from the network is more than 50%. Therefore, the final SoC of batteries at departure time is considered in the range of [0.5,1].

In each scenario, for further comparison, the cost function suggested in [30], [31], and [32] is used for the load curve flattening as follows:

$$\Delta P_t = \left| \sum_{i=1}^{N(t)} p_i^{D,t} - \sum_{i=1}^{N(t)} p_i^{PV,t} - \sum_{i=1}^{N(t)} p_i^{WT,t} + \gamma_n \left(\sum_{i=1}^{N(t)} q_i^{C,t} - \sum_{i=1}^{N(t)} q_i^{D,t} \right) - p_{grid}^{spec} \right| \quad (10)$$

where p_{grid}^{spec} is the specified grid power and is considered as the average of the load curve. Equation (10) is used for the load curve flattening per hour t. The total cost function for time interval t is obtained by adding the battery degradation cost (6) to (10) as follows:

$$C = \Delta P_t + \gamma_n H_n(q_n^t) \quad (11)$$

The simulation result of Scenario 1 with Equation (7) which is obtained by implementing the modified algorithm is shown in Fig. 4. In Fig. 4 to 9, the light bars represent the total power consumption, the dark bars represent the total battery charge, and the dashed-line curve represents the load profile. The horizontal axis represents 24 hours a day.

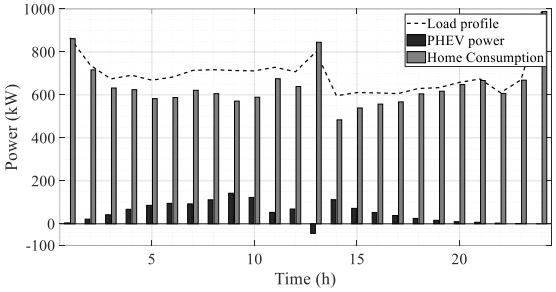

Fig. 4 Total battery charge, total home load, and total system load curve in Scenario 1 with Equation (7).

Tables 4 to 6 show a typical vehicle of different types with different requests and show their battery charge 24 hours a day. Tables 4 to 6 show that the aggregator optimizes battery charging 24 hours a day by satisfying car requests in Equation (7) with Scenarios 1 to 3, respectively. Also, the daily bill and the cost of battery depreciation are given at the end of the tables.

Table 3 Details of each scenario.

	Scenario 1	Scenario 2	Scenario 3
Total number of customers	110	220	330
Average number of each type of vehicle	10	20	30
Total number of home loads	0.6*110=66	0.5*220=110	0.7*330=231
Homes with PV	(3/6)*66=33	0.2*110=22	(1/3)*231=77
Homes with WT	(2/6)*66=22	0.2*110=22	(1/3)*231=77
Homes without renewable resources	(1/6)*66=11	0.1*110=11	(1/3)*231=77
Vehicles in parking lots	0.4*110=44	0.5*220=110	0.3*330=99
Arrival time (randomly in the interval)	[1,10]	[1,6]	[1,14]
Departure time (randomly in the interval)	[13,24]	[9,24]	[17,24]

Table 4 Optimal battery charge 24 hours a day based on their request with Equation (7) in Scenario 1.

Types of vehicles	Chevrolet	Honda	Fiat	BMW	Mercedes	Ford	Hyundai	Nissan	Toyota	Kia	Tesla
initial SoC	0.9382	0.7764	0.7571	0.7567	0.9281	0.9206	0.9444	0.8959	0.9250	0.5785	0.4437
final SoC	0.6416	0.9339	0.5937	0.7399	0.9236	0.6812	0.5649	0.9782	0.7472	0.6378	0.6459
arrival time	7	7	8	3	5	8	4	7	5	8	9
departure time	20	13	21	14	15	17	18	17	18	21	19
charge at hour 1	0.9382	0.7764	0.7571	0.7567	0.9281	0.9206	0.9444	0.8959	0.9250	0.5785	0.4437
charge at hour 2	0.9382	0.7764	0.7571	0.7567	0.9281	0.9206	0.9444	0.8959	0.9250	0.5785	0.4437
charge at hour 3	0.9382	0.7764	0.7571	0.7567	0.9281	0.9206	0.9444	0.8959	0.9250	0.5785	0.4437
charge at hour 4	0.9382	0.7764	0.7571	0.7567	0.9281	0.9206	0.9095	0.8959	0.9250	0.5785	0.4437
charge at hour 5	0.9382	0.7764	0.7571	0.7755	0.9281	0.9206	0.8875	0.8959	0.9184	0.5785	0.4437
charge at hour 6	0.9382	0.7764	0.7571	0.7815	0.9281	0.9206	0.8683	0.8959	0.9118	0.5785	0.4437
charge at hour 7	0.9382	0.8029	0.7571	0.7815	0.9281	0.9206	0.8401	0.8981	0.8903	0.5785	0.4437
charge at hour 8	0.9382	0.8530	0.7571	0.7823	0.9281	0.9106	0.8169	0.9035	0.8842	0.5792	0.4437
charge at hour 9	0.9382	0.9232	0.7571	0.7944	0.9376	0.9106	0.8097	0.9144	0.8842	0.5925	0.4703
charge at hour 10	0.9382	0.9752	0.7571	0.8065	0.9423	0.9055	0.7885	0.9223	0.8822	0.5960	0.4912
charge at hour 11	0.8763	0.9752	0.7103	0.8007	0.9301	0.8497	0.7410	0.9223	0.8515	0.5960	0.4943
charge at hour 12	0.8316	1.0000	0.6878	0.8017	0.9301	0.8079	0.7067	0.9223	0.8274	0.5974	0.5110
charge at hour 13	0.6168	0.9339	0.5316	0.6948	0.8317	0.6779	0.5931	0.8584	0.7336	0.5494	0.4922
charge at hour 14	0.6600	0.9339	0.5753	0.7399	0.8867	0.6812	0.6076	0.9013	0.7626	0.5729	0.5297
charge at hour 15	0.6600	0.9339	0.6035	0.7399	0.9236	0.6812	0.6076	0.9322	0.7626	0.5944	0.5618
charge at hour 16	0.6667	0.9339	0.6242	0.7399	0.9236	0.6812	0.6050	0.9575	0.7626	0.6123	0.5827
charge at hour 17	0.6678	0.9339	0.6247	0.7399	0.9236	0.6812	0.5900	0.9782	0.7626	0.6272	0.6106
charge at hour 18	0.6678	0.9339	0.6247	0.7399	0.9236	0.6812	0.5649	0.9782	0.7472	0.6378	0.6305
charge at hour 19	0.6678	0.9339	0.6247	0.7399	0.9236	0.6812	0.5649	0.9782	0.7472	0.6378	0.6459
charge at hour 20	0.6416	0.9339	0.6129	0.7399	0.9236	0.6812	0.5649	0.9782	0.7472	0.6378	0.6459
charge at hour 21	0.6416	0.9339	0.5937	0.7399	0.9236	0.6812	0.5649	0.9782	0.7472	0.6378	0.6459
charge at hour 22	0.6416	0.9339	0.5937	0.7399	0.9236	0.6812	0.5649	0.9782	0.7472	0.6378	0.6459
charge at hour 23	0.6416	0.9339	0.5937	0.7399	0.9236	0.6812	0.5649	0.9782	0.7472	0.6378	0.6459
charge at hour 24	0.6416	0.9339	0.5937	0.7399	0.9236	0.6812	0.5649	0.9782	0.7472	0.6378	0.6459
daily bill	2327111	2432895	2378960	2314514	2353698	2284007	2115215	2440015	2233247	2417383	2688417
cost of battery degradation	19.9493	7.9797	19.6272	11.8643	13.0384	26.6090	33.9436	15.7587	23.0552	20.3212	48.6414

The simulation result of Scenario 1 with Equation (11) which is obtained by implementing the modified algorithm is shown in Fig. 5.

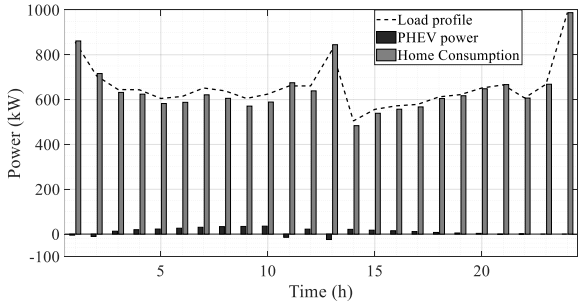

Fig. 5 Total battery charge, total home load, and total system load curve in Scenario 1 with Equation (11).

The simulation result of Scenario 2 with Equation (7) which is obtained by implementing the modified algorithm is shown in Fig. 6.

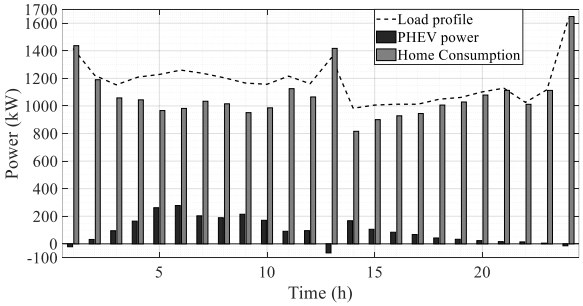

Fig. 6 Total battery charge, total home load, and total system load curve in Scenario 2 with Equation (7).

Table 5 Optimal battery charge 24 hours a day based on their request with Equation (7) in Scenario 2.

Types of vehicles	Chevrolet	Honda	Fiat	BMW	Mercedes	Ford	Hyundai	Nissan	Toyota	Kia	Tesla
initial SoC	0.6634	0.6332	0.4379	0.8126	0.7593	0.7417	0.6734	0.5860	0.9350	0.6832	0.5363
final SoC	0.7536	0.6461	0.9039	0.7568	0.7931	0.9634	0.8339	0.6137	0.7422	0.8447	0.6668
arrival time	5	5	1	3	6	1	4	6	3	2	4
departure time	22	20	17	21	24	19	14	21	20	15	15
charge at hour 1	0.6634	0.6332	0.4379	0.8126	0.7593	0.7417	0.6734	0.5860	0.9350	0.6832	0.5363
charge at hour 2	0.6634	0.6332	0.4379	0.8126	0.7593	0.7287	0.6734	0.5860	0.9350	0.6832	0.5363
charge at hour 3	0.6634	0.6332	0.4515	0.8126	0.7593	0.7287	0.6734	0.5860	0.9160	0.6856	0.5363
charge at hour 4	0.6634	0.6332	0.4553	0.8126	0.7593	0.7287	0.6800	0.5860	0.9095	0.6959	0.5465
charge at hour 5	0.6758	0.6332	0.5097	0.8200	0.7593	0.7487	0.7062	0.5860	0.9095	0.7186	0.5655
charge at hour 6	0.6839	0.6391	0.5597	0.8230	0.7661	0.7666	0.7275	0.5921	0.9034	0.7355	0.5814
charge at hour 7	0.6839	0.6391	0.5887	0.8230	0.7668	0.7666	0.7352	0.5921	0.8859	0.7463	0.5911
charge at hour 8	0.6839	0.6391	0.6222	0.8230	0.7843	0.7715	0.7544	0.5927	0.8838	0.7596	0.6038
charge at hour 9	0.7005	0.6525	0.6674	0.8333	0.7992	0.8057	0.7851	0.5987	0.8838	0.7835	0.6245
charge at hour 10	0.7014	0.6525	0.7122	0.8333	0.8192	0.8249	0.8094	0.5987	0.8838	0.8032	0.6377
charge at hour 11	0.7014	0.6340	0.7122	0.8112	0.8192	0.8249	0.8094	0.5949	0.8516	0.8032	0.6377
charge at hour 12	0.7014	0.6340	0.7326	0.8085	0.8192	0.8249	0.8135	0.5949	0.8358	0.8110	0.6395
charge at hour 13	0.5615	0.5024	0.6313	0.6761	0.7510	0.7683	0.7685	0.5149	0.7493	0.7784	0.6119
charge at hour 14	0.6657	0.5896	0.7162	0.7153	0.8319	0.8417	0.8339	0.5504	0.7785	0.8144	0.6456
charge at hour 15	0.7036	0.6182	0.7831	0.7363	0.8871	0.8887	0.8339	0.5762	0.7785	0.8447	0.6668
charge at hour 16	0.7517	0.6423	0.8483	0.7520	0.9296	0.9222	0.8339	0.5994	0.7785	0.8447	0.6668
charge at hour 17	0.7706	0.6518	0.9039	0.7609	0.9527	0.9473	0.8339	0.6137	0.7785	0.8447	0.6668
charge at hour 18	0.7706	0.6518	0.9039	0.7609	0.9592	0.9577	0.8339	0.6137	0.7739	0.8447	0.6668
charge at hour 19	0.7706	0.6518	0.9039	0.7609	0.9594	0.9634	0.8339	0.6137	0.7648	0.8447	0.6668
charge at hour 20	0.7706	0.6461	0.9039	0.7602	0.9594	0.9634	0.8339	0.6137	0.7422	0.8447	0.6668
charge at hour 21	0.7536	0.6461	0.9039	0.7568	0.9594	0.9634	0.8339	0.6137	0.7422	0.8447	0.6668
charge at hour 22	0.7536	0.6461	0.9039	0.7568	0.9656	0.9634	0.8339	0.6137	0.7422	0.8447	0.6668
charge at hour 23	0.7536	0.6461	0.9039	0.7568	0.9656	0.9634	0.8339	0.6137	0.7422	0.8447	0.6668
charge at hour 24	0.7536	0.6461	0.9039	0.7568	0.7931	0.9634	0.8339	0.6137	0.7422	0.8447	0.6668
daily bill	2383668.6	2357584.8	2560159	2404088	2353112.7	2429988	2472276	2425875.3	2192267.3	2584857.7	2638650.7
cost of battery degradation	14.0870	12.6208	35.2500	16.8761	42.7321	29.5880	17.7343	16.9321	21.1295	28.8642	30.6655

The simulation result of Scenario 2 with Equation (11) which is obtained by implementing the modified algorithm is shown in Fig. 7.

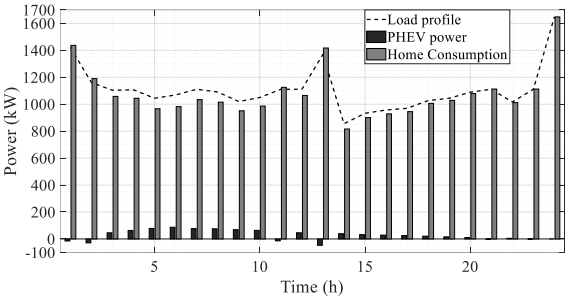

Fig. 7 Total battery charge, total home load, and total system load curve in Scenario 2 with Equation (11).

The simulation result of Scenario 3 with Equation (7) which is obtained by implementing the modified algorithm is shown in Fig. 8. The simulation result of Scenario 3 with Equation (11) which is obtained by implementing the modified algorithm is shown in Fig. 9. Given that the load profile in Figures 4, 6, and 8 is without peak and valley; therefore, the load profile is relatively smooth. In addition to smoothing the load curve, our goal was to minimize the daily bill and the cost of battery degradation. This is why, by minimizing the cost function, the load profile is not completely smoothed yet.

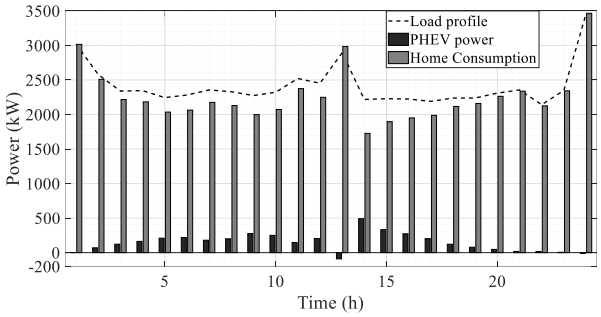

Fig. 8 Total battery charge, total home load, and total system load curve in Scenario 3 with Equation (7).

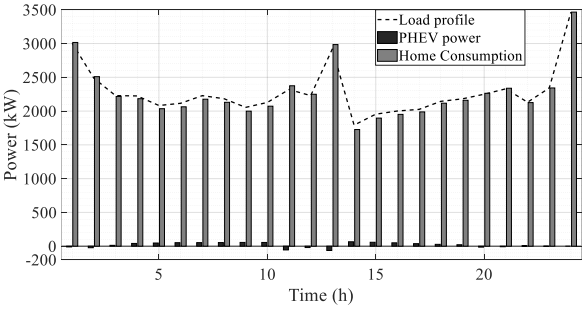

Fig. 9 Total battery charge, total home load, and total system load curve in Scenario 3 with Equation (11).

Table 6 Optimal battery charge 24 hours a day based on their request with Equation (7) in Scenario 3.

Types of vehicles	Chevrolet	Honda	Fiat	BMW	Mercedes	Ford	Hyundai	Nissan	Toyota	Kia	Tesla
initial SoC	0.7086	0.6347	0.7070	0.3569	0.9696	0.6250	0.6733	0.8484	0.5520	0.5958	0.5750
final SoC	0.6265	0.5991	0.9443	0.7733	0.5478	0.7308	0.7076	0.8830	0.5897	0.7157	0.9734
arrival time	7	13	11	10	9	11	8	12	13	13	14
departure time	17	20	19	20	19	20	17	21	17	18	24
charge at hour 1	0.7086	0.6347	0.7070	0.3569	0.9696	0.6250	0.6733	0.8484	0.5520	0.5958	0.5750
charge at hour 2	0.7086	0.6347	0.7070	0.3569	0.9696	0.6250	0.6733	0.8484	0.5520	0.5958	0.5750
charge at hour 3	0.7086	0.6347	0.7070	0.3569	0.9696	0.6250	0.6733	0.8484	0.5520	0.5958	0.5750
charge at hour 4	0.7086	0.6347	0.7070	0.3569	0.9696	0.6250	0.6733	0.8484	0.5520	0.5958	0.5750
charge at hour 5	0.7086	0.6347	0.7070	0.3569	0.9696	0.6250	0.6733	0.8484	0.5520	0.5958	0.5750
charge at hour 6	0.7086	0.6347	0.7070	0.3569	0.9696	0.6250	0.6733	0.8484	0.5520	0.5958	0.5750
charge at hour 7	0.7086	0.6347	0.7070	0.3569	0.9696	0.6250	0.6733	0.8484	0.5520	0.5958	0.5750
charge at hour 8	0.7086	0.6347	0.7070	0.3569	0.9696	0.6250	0.6767	0.8484	0.5520	0.5958	0.5750
charge at hour 9	0.7278	0.6347	0.7070	0.3569	0.9584	0.6250	0.6866	0.8484	0.5520	0.5958	0.5750
charge at hour 10	0.7278	0.6347	0.7070	0.4038	0.9459	0.6250	0.6929	0.8484	0.5520	0.5958	0.5750
charge at hour 11	0.6818	0.6347	0.7070	0.4139	0.8739	0.6250	0.6913	0.8484	0.5520	0.5958	0.5750
charge at hour 12	0.6818	0.6347	0.7070	0.4413	0.8151	0.6250	0.6913	0.8484	0.5520	0.5958	0.5750
charge at hour 13	0.4926	0.4908	0.6286	0.3784	0.6670	0.5485	0.6163	0.7849	0.4901	0.5766	0.5750
charge at hour 14	0.5465	0.5672	0.7414	0.4720	0.6754	0.6066	0.6581	0.8403	0.5390	0.6199	0.6389
charge at hour 15	0.5761	0.5958	0.8079	0.5468	0.6754	0.6435	0.6794	0.8583	0.5628	0.6530	0.6940
charge at hour 16	0.6035	0.6098	0.8612	0.6098	0.6649	0.6736	0.6892	0.8765	0.5776	0.6832	0.7451
charge at hour 17	0.6265	0.6098	0.9086	0.6711	0.6437	0.6986	0.7076	0.8888	0.5897	0.7067	0.7926
charge at hour 18	0.6265	0.6098	0.9286	0.7196	0.5987	0.7139	0.7076	0.8888	0.5897	0.7157	0.8298
charge at hour 19	0.6265	0.6098	0.9443	0.7582	0.5478	0.7282	0.7076	0.8888	0.5897	0.7157	0.8690
charge at hour 20	0.6265	0.5991	0.9443	0.7733	0.5478	0.7308	0.7076	0.8888	0.5897	0.7157	0.8988
charge at hour 21	0.6265	0.5991	0.9443	0.7733	0.5478	0.7308	0.7076	0.8830	0.5897	0.7157	0.9265
charge at hour 22	0.6265	0.5991	0.9443	0.7733	0.5478	0.7308	0.7076	0.8830	0.5897	0.7157	0.9654
charge at hour 23	0.6265	0.5991	0.9443	0.7733	0.5478	0.7308	0.7076	0.8830	0.5897	0.7157	0.9904
charge at hour 24	0.6265	0.5991	0.9443	0.7733	0.5478	0.7308	0.7076	0.8830	0.5897	0.7157	0.9734
daily bill	2412909.9	2337965.9	2455084.9	2576939.3	2168316.8	2517623.9	2371980	2386023.2	2398280.3	2506481.3	3055400.3
daily cost of battery degradation	16.1737	12.6584	21.3535	31.9025	30.6476	17.1208	14.3622	15.2925	14.9822	26.2262	153.2483

To compare the results of optimization using Equations (7) and (11), the variance and average load curve and simulation time of these two methods in three different scenarios are given in Table 7. In all three scenarios, the simulation time and the variance load curve resulting from equation (7) are less than the simulation time and the variance load curve resulting from equation (11). As a result, the optimization results from equation (7) have reduced both the variance load curve and the simulation time, and met the customer requirements.

5 Conclusions

Different connection strategies of electric vehicle batteries in homes and parking lots were examined. The output power of home-installed small wind turbines and photovoltaics using the forecast based on the previous days has been applied in the optimization. The modified algorithm met the total vehicle demands well, and it smoothed the load curve. Using the proposed algorithm, both the profit of the distribution network and the customers are maximized. In addition, the predetermined battery charge is met when disconnecting the vehicle from the network.

Intellectual Property

The authors confirm that they have given due consideration to the protection of intellectual property associated with this work and that there are no impediments to publication, including the timing to publication, with respect to intellectual property.

Funding

No funding was received for this work.

CRediT Authorship Contribution Statement

V. Bagheri: Idea & Conceptualization**,** Research & Investigation**,** Analysis**,** Methodology**,** Software and Simulation**,** Original Draft Preparation**,** Revise & Editing**. A. F. Ehyaei:** Idea & Conceptualization, Methodology**,** Project Administration**,** Supervision**,** Verification**,** Revise & Editing**. M. Haeri:** Idea & Conceptualization, Methodology, Project Administration, Supervision**,** Verification, Revise & Editing.

Table 7 Comparison between optimization with Equations (7) and (11) in different scenarios.

	Scenario 1	Scenario 2	Scenario 3
Load curve variance with Equation (7)	7899.26	21755.22	92489.61
Load curve average with Equation (7)	695.79	1171.39	2412.92
Simulation time with Equation (7) (mins)	18.45	38.99	51.57
Load curve variance with Equation (11)	10441.38	27603.05	134325.32
Load curve average with Equation (11)	656.74	1105.51	2284.25
Simulation time with Equation (11) (mins)	23.87	55.16	81.79

Declaration of Competing Interest

The authors hereby confirm that the submitted manuscript is an original work and has not been published so far, is not under consideration for publication by any other journal and will not be submitted to any other journal until the decision will be made by this journal. All authors have approved the manuscript and agree with its submission to "Iranian Journal of Electrical and Electronic Engineering"

References

[1] T. Logenthiran, D. Srinivasan, and T. Z. Shun, "Demand side management in smart grid using heuristic optimization," IEEE Transactions on Smart Grid, Vol. 3, No. 3, pp. 1244-1252, 2012.

[2] E. Sarker, P. Halder, M. Seyedmahmoudian, E. Jamei, B. Horan, S. Mekhilef, and A. Stojcevski, "Progress on the demand side management in smart grid and optimization approaches," *International Journal of Energy Research*, Vol. 45, No. 1, pp. 36-64, 2021.

[3] R. Dharani, M. Balasubramonian, T.S. Babu, and B. Nastasi, "Load shifting and peak clipping for reducing energy consumption in an Indian University Campus," *Energies*, Vol. 14, No. 3, 558, 2021.

[4] R. Sebastián, "Application of a battery energy storage for frequency regulation and peak shaving in a wind diesel power system," *IET Generation, Transmission & Distribution*, Vol. 10, No. 3, pp. 764-770, 2016.

[5] E. Guelpa, G. Barbero, A. Sciacovelli, and V. Verda, "Peak-shaving in district heating systems through optimal management of the thermal request of buildings," *Energy*, Vol. 137, pp. 706-714, 2017.

[6] A. J. Pimm, T. T. Cockerill, and P. G. Taylor, "The potential for peak shaving on low voltage distribution networks using electricity storage," *Journal of Energy Storage*, Vol. 16, pp. 231-242, 2018.

[7] E. Reihani, M. Motalleb, R. Ghorbani, and L.S. Saoud, "Load peak shaving and power smoothing of a distribution grid with high renewable energy penetration," *Renewable Energy*, Vol. 86, pp. 1372-1379, 2016.

[8] R. Luthander, J. Widén, J. Munkhammar, and D. Lingfors, "Self-consumption enhancement and peak shaving of residential photovoltaics using storage and curtailment," *Energy*, Vol. 112, pp. 221-231, 2016.

[9] R. Martins, H. C. Hesse, J. Jungbauer, T. Vorbuchner, and P. Musilek, "Optimal component sizing for peak shaving in battery energy storage system for industrial applications," *Energies*, Vol. 11, No. 8, 2048, 2018.

[10] K. H. Chua, Y. S. Lim, and S. Morris, "Energy storage system for peak shaving," *International Journal of Energy Sector Management*, Vol. 10, No. 1, pp. 3-18, 2016.

[11] S. Chapaloglou, A. Nesiadis, P. Iliadis, K. Atsonios, N. Nikolopoulos, P. Grammelis, C. Yiakopoulos, I. Antoniadis, and E. Kakaras, "Smart energy management algorithm for load smoothing and peak shaving based on load forecasting of an island's power system," *Applied Energy*, Vol. 238, pp. 627-642, 2019.

[12] Y. Shi, B. Xu, D. Wang, and B. Zhang, "Using battery storage for peak shaving and frequency regulation: Joint optimization for super-linear gains," *IEEE Transactions on Power Systems*, Vol. 33, No. 3, pp. 2882-2894, 2017.

[13] E. Shirazi and S. Jadid, "Cost reduction and peak shaving through domestic load shifting and DERs," *Energy*, Vol. 124, pp. 146-159, 2017.

[14] H. Liang, Y. Liu, F. Li, and Y. Shen, "Dynamic economic/emission dispatch including PEVs for peak shaving and valley filling," *IEEE Transactions on Industrial Electronics*, Vol. 66, No. 4, pp. 2880-2890, 2018.

[15] L. Jian, Y. Zheng, and Z. Shao, "High efficient valley-filling strategy for centralized coordinated charging of large-scale electric vehicles," *Applied Energy*, Vol. 186, pp. 46-55, 2017.

[16] C. S. Ioakimidis, D. Thomas, P. Rycerski, and K. N. Genikomsakis, "Peak shaving and valley

filling of power consumption profile in non-residential buildings using an electric vehicle parking lot," *Energy*, Vol. 148, pp. 148-158, 2018.

[17] Z. Hu, K. Zhan, H. Zhang, and Y. Song, "Pricing mechanisms design for guiding electric vehicle charging to fill load valley," *Applied Energy*, Vol. 178, pp. 155-163, 2016.

[18] M. Yu and S. H. Hong, "Supply–demand balancing for power management in smart grid: A Stackelberg game approach," *Applied Energy*, Vol. 164, pp. 702-710, 2016.

[19] C. Li, X. Yu, W. Yu, G. Chen, and J. Wang, "Efficient computation for sparse load shifting in demand side management," *IEEE Transactions on Smart Grid*, Vol. 8, No. 1, pp. 250-261, 2016.

[20] E. Reihani, S. Sepasi, L. R. Roose, and M. Matsuura, "Energy management at the distribution grid using a Battery Energy Storage System (BESS)," *International Journal of Electrical Power & Energy Systems*, Vol. 77, pp. 337-344, 2016.

[21] G. Graditi, M. G. Ippolito, E. Telaretti, and G. Zizzo, "Technical and economical assessment of distributed electrochemical storages for load shifting applications: An Italian case study," *Renewable and Sustainable Energy Reviews*, Vol. 57, pp. 515-523, 2016.

[22] C. C. Lin, D. J. Deng, W. Y. Liu, and L. Chen, "Peak load shifting in the internet of energy with energy trading among end-users," *IEEE Access*, Vol. 5, pp. 1967-1976, 2017.

[23] S. Feuerriegel and D. Neumann, "Integration scenarios of demand response into electricity markets: Load shifting, financial savings and policy implications," *Energy Policy*, Vol. 96, pp. 231-240, 2016.

[24] S. Khemakhem, M. Rekik, and L. Krichen, "A flexible control strategy of plug-in electric vehicles operating in seven modes for smoothing load power curves in smart grid," *Energy*, Vol. 118, pp. 197-208, 2017.

[25] M. Shokri and H. Kebriaei, "Mean-field optimal energy management of plug-in hybrid electric vehicles," *IEEE Transactions on Vehicular Technology*, Vol. 68, No. 1, pp. 113-120, 2018.

[26] V. Berinde and F. Takens, *Iterative Approximation of Fixed Points*, Vol. 1912, Berlin: Springer, 2007.

[27] A. Safdarian, M. Z. Degefa, M. Lehtonen, and M. Fotuhi-Firuzabad, "Distribution network reliability improvements in presence of demand response," *IET Generation, Transmission & Distribution*, Vol. 8, No. 12, pp. 2027-2035, 2014.

[28] A. A. Moghaddam, A. Seifi, T. Niknam, and M.R.A. Pahlavani, "Multi-objective operation management of a renewable MG (micro-grid) with back-up micro-turbine/fuel cell/battery hybrid power source," *Energy*, Vol. 36, No. 11, pp. 6490-6507, 2011.

[29] Y. Jin, B. Yu, M. Seo, and S. Han, "Optimal aggregation design for massive V2G participation in energy market," *IEEE Access*, Vol. 8, 211794-211808, 2020.

[30] K. R. Reddy and S. Meikandasivam, "Load flattening and voltage regulation using plug-in electric vehicle's storage capacity with vehicle prioritization using anfis", *IEEE Transactions on Sustainable Energy*, Vol. 11, No. 1, pp. 260-270, 2018.

[31] K. R. Reddy, S. Meikandasivam, and D. Vijayakumar, "A novel strategy for maximization of plug-in electric vehicle's storage utilization for grid support with consideration of customer flexibility", *Electric Power Systems Research*, Vol. 170, pp. 158-175, 2019.

[32] S. Meikandasivam, "Optimal distribution of plug-in-electric vehicle's storage capacity using water filling algorithm for load flattening and vehicle prioritization using ANFIS", *Electric Power Systems Research*, Vol. 165, pp. 120-133, 2018.

Vahid Bagheri received the B.Sc. degree in electrical control engineering from Shahed University, Tehran, Iran, in 2014. He received the M.Sc. degree in electrical control engineering from Qom University, Qom, Iran, in 2016. He received the Ph.D. degree in electrical control engineering from Imam Khomeini International University, Qazvin, Iran, in 2022.

Amir Farhad Ehyaei received the B.Sc. degree in electrical and electronics engineering from Sharif University of Technology, Tehran, Iran, in 2001. He received the M.Sc. and Ph.D. degrees both in electrical engineering from Iran University of Science and Technology, Tehran, Iran, in 2003 and 2011, respectively. Since 2011, he has been with the Faculty of Electrical Engineering, Imam Khomeini International University, Qazvin, Iran.

Mohammad Haeri received the B.Sc. and M.Sc. degrees both in electrical engineering from Amirkabir University of Technology, Tehran, Iran, in 1985 and 1988, respectively. He received the Ph.D. degree in electrical engineering from University of Saskatchewan, Canada, in 1994. Since 1994, he has been with the Electrical Engineering Department, Sharif University of Technology, Iran, where he is now Professor and Head of the Advanced Control System Lab.

© 2022 by the authors. Licensee IUST, Tehran, Iran. This article is an open-access article distributed under the terms and conditions of the Creative Commons Attribution-NonCommercial 4.0 International (CC BY-NC 4.0)
license (https://creativecommons.org/licenses/by-nc/4.0/).